Supplemental Information

Gelatin-based hydrogel degradation and tissue interaction *in vivo*: insights from multimodal preclinical imaging in immunocompetent nude mice

Christoph Tondera[1,2], Sandra Hauser[1], Anne Krüger-Genge[3], Friedrich Jung[3,4], Axel T. Neffe[3,4], Andreas Lendlein[3,4], Robert Klopfleisch[5], Jörg Steinbach[2,6], Christin Neuber[1], Jens Pietzsch[1,2,*]

[1]Helmholtz-Zentrum Dresden-Rossendorf, Institute of Radiopharmaceutical Cancer Research, Department of Radiopharmaceutical and Chemical Biology, Dresden, Germany

[2]Technische Universität Dresden, Department of Chemistry and Food Chemistry, Dresden, Germany

[3]Institute of Biomaterial Science and Berlin-Brandenburg Centre for Regenerative Therapies, Helmholtz-Zentrum Geesthacht, Teltow, Germany

[4]Helmholtz Virtual Institute "Multifunctional Biomaterials for Medicine", Teltow and Berlin

[5]Freie Universität Berlin, Institute of Veterinary Pathology, Berlin, Germany

[6]Helmholtz-Zentrum Dresden-Rossendorf, Institute of Radiopharmaceutical Cancer Research, Dresden, Germany

*Corresponding author: Tel.: +49 351 260 2622. j.pietzsch@hzdr.de (J. Pietzsch)

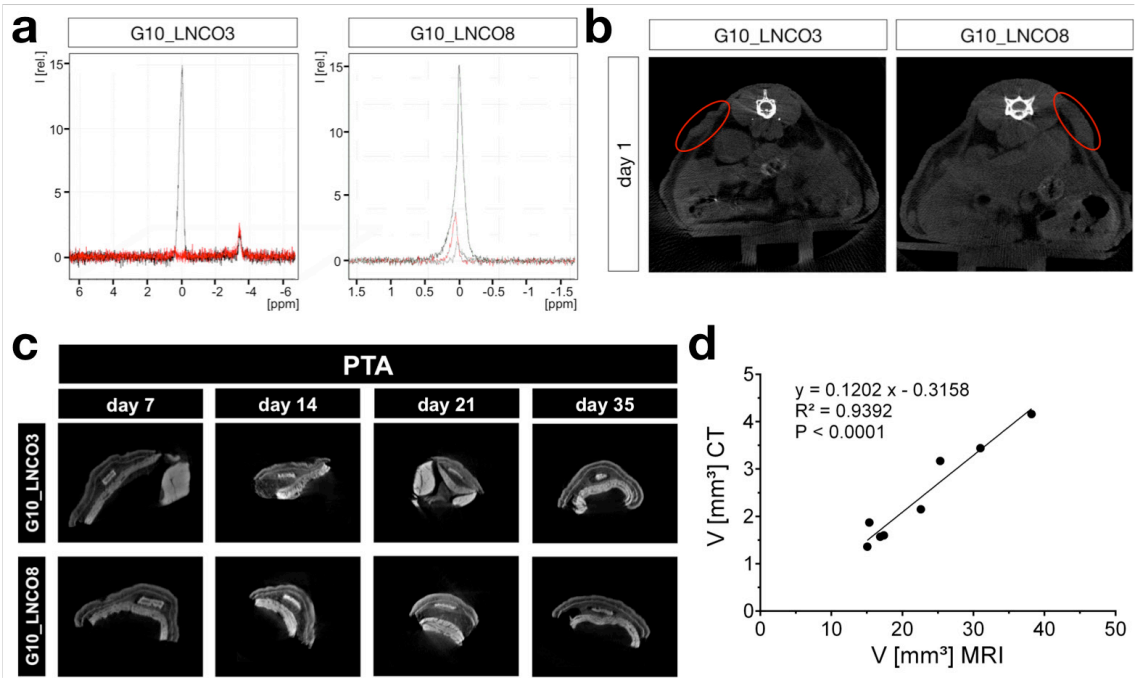

Fig. S1 Methodological evaluation of hydrogel imaging and quantification. (a) Spectral MRI measurement of G10_LNCO3 and G10_LNCO8 without (black) and with water peak suppression (red) in case of G10_LNCO3 and with different volume of interest sizes (red: higher volume, black: smaller volume) in case of G10_LNCO8. (b) *In vivo* CT measurement of implanted animals 1 day after implantation. (c) *Ex vivo* CT measurement of explanted hydrogel-tissue samples after 49 days of PTA staining and (d) the correlation between volume quantified using MRI *in vivo* compared to the quantification after the PTA staining and CT measurement *ex vivo*.

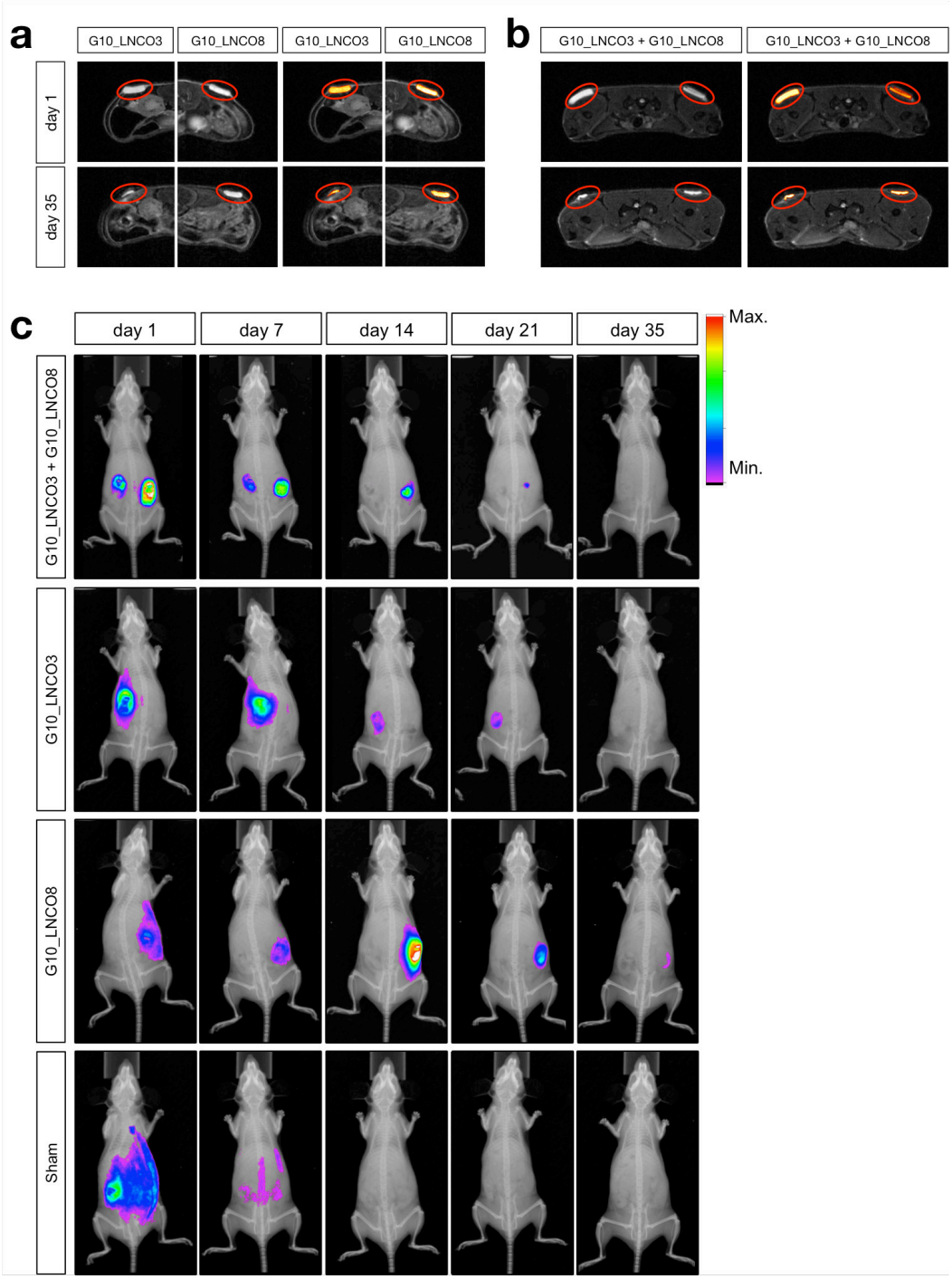

Fig. S2 MRI images and optical imaging of MMP activity of single- and double-implanted animals. Representative axial MRI images of G10_LNCO3 or G10_LNCO8 in (a) single-implanted (compare Fig. 1b) or (b) double-implanted animals on day 1 and day 35 after implantation. After drawing a volume of interest around the hydrogel (red sphere) and applying a threshold (a and b right panel) the volume of the hydrogels could be calculated. (c) Representative fluorescence images of *in vivo* MMP activity measurements using MMP-Sense 680. Double-implanted, single-implanted and sham-operated animals are shown.

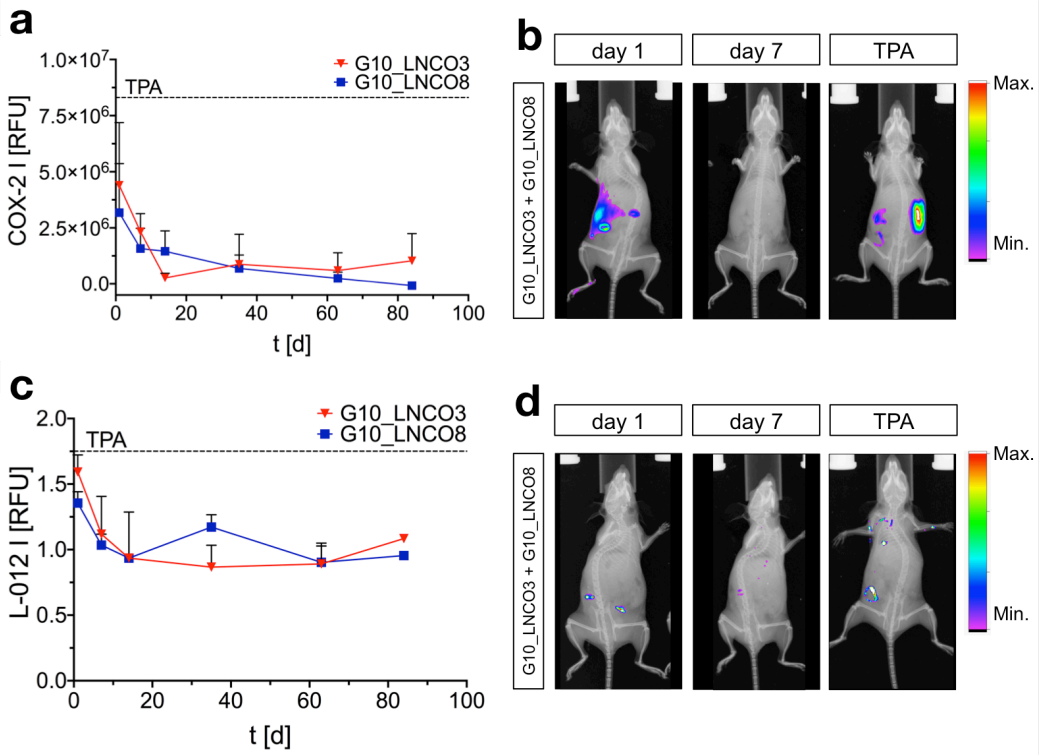

Fig. S3 Optical imaging and quantification COX-2 synthesis and ROS production (L-012). (a) Quantification of signal accumulation of the fluorescent COX-2 tracer and (b) representative fluorescence images. (c) Quantification of signal accumulation of the luminescent ROS detecting agent and (d) representative fluorescence images. Comparison to animals with induced inflammation after injection of TPA. Measurements were performed with double-implanted animals. Except for the incision site no signal of both imaging agents could be detected. Mean + s.d.

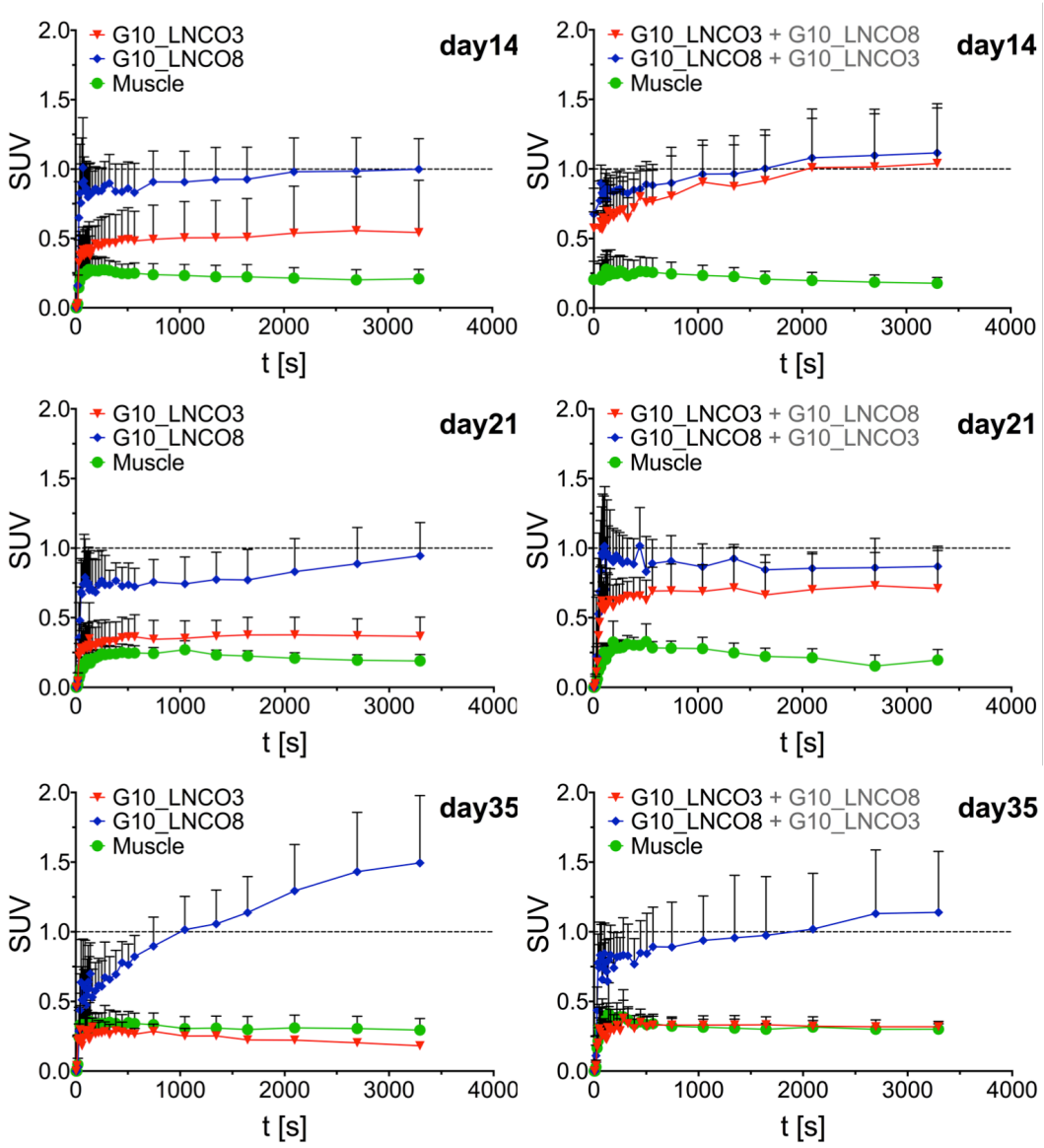

Fig. S4 Time-activity curves of [^{18}F]FDG uptake. Time-activity curves [^{18}F]FDG uptake are shown 14, 21, and 35 days after implantation of G10_LNCO3 and G10_LNCO8 in single-implanted (left panel) and double-implanted (right panel) mice (mean SUV + s.d.).

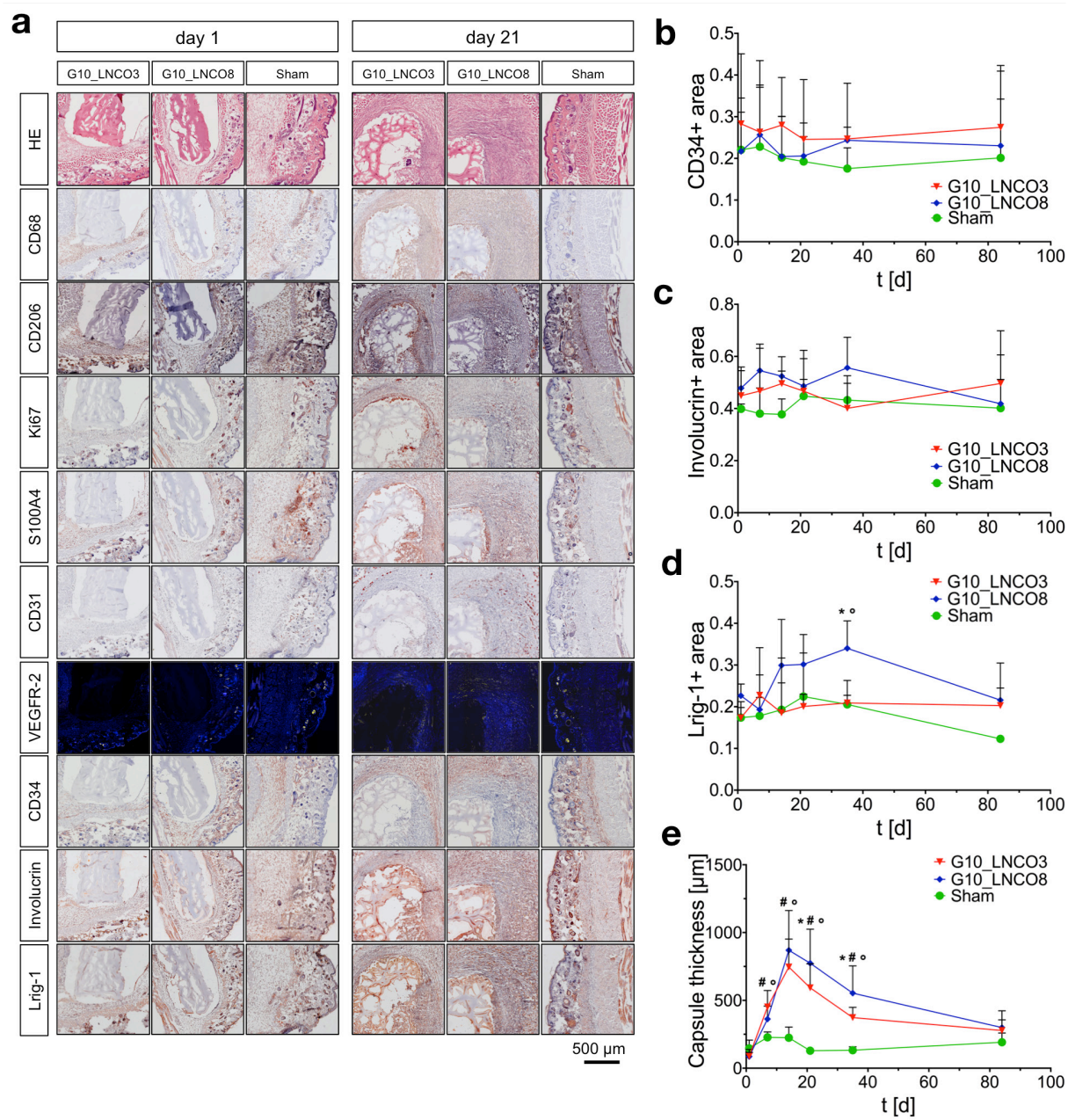

Fig. S5 Representative histological images and quantification of involucrin, Lrig-1, and capsule thickness. (a) Representative histological images 1 day (left panel) and 21 days (right panel) after implantation. Histological quantification of positive stained area compared to counterstaining of cell nuclei of single-implanted animals. Course of time shown for (b) fibrocyte marker CD34, (c) keratinocyte marker involucrin, and (d) fibroblast stem cell marker Lrig-1 (n=3 different animals). Quantification was applied using color thresholds at mosaic images of whole, centric 10 µm slices of the hydrogel implant and the surrounding tissue. (e) Capsule thickness around the hydrogel compared to sham-operated animals (n=3 different animals, 5 measuring points per implant site (skin or muscle) and per animal). Error bars, mean + s.d. * G10_LNCO3 vs. G10_LNCO8, # G10_LNCO3 vs. Sham, ° G10_LNCO8 vs. Sham $p < 0.1$.

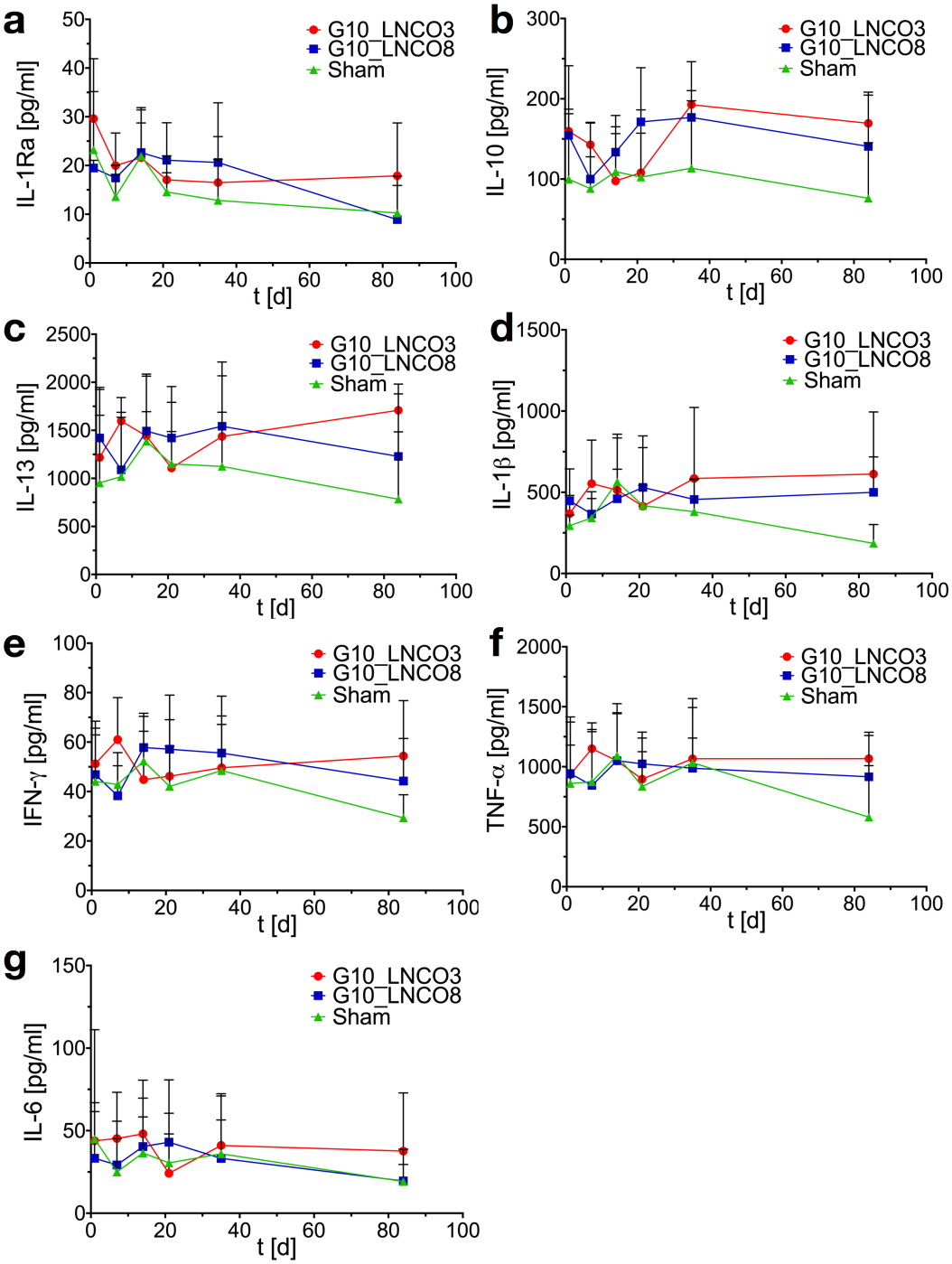

Fig. S6 Serum cytokine quantification. Time course of anti-inflammatory cytokines (a) IL-1Ra, (b) IL-10, (c) IL-13 and pro-inflammatory cytokines (d) IL-1β, (e) IFN-γ, (f) TNF-α, and (g) IL-6 in serum of single-implanted mice (n=4 different animals, mean + s.d.).

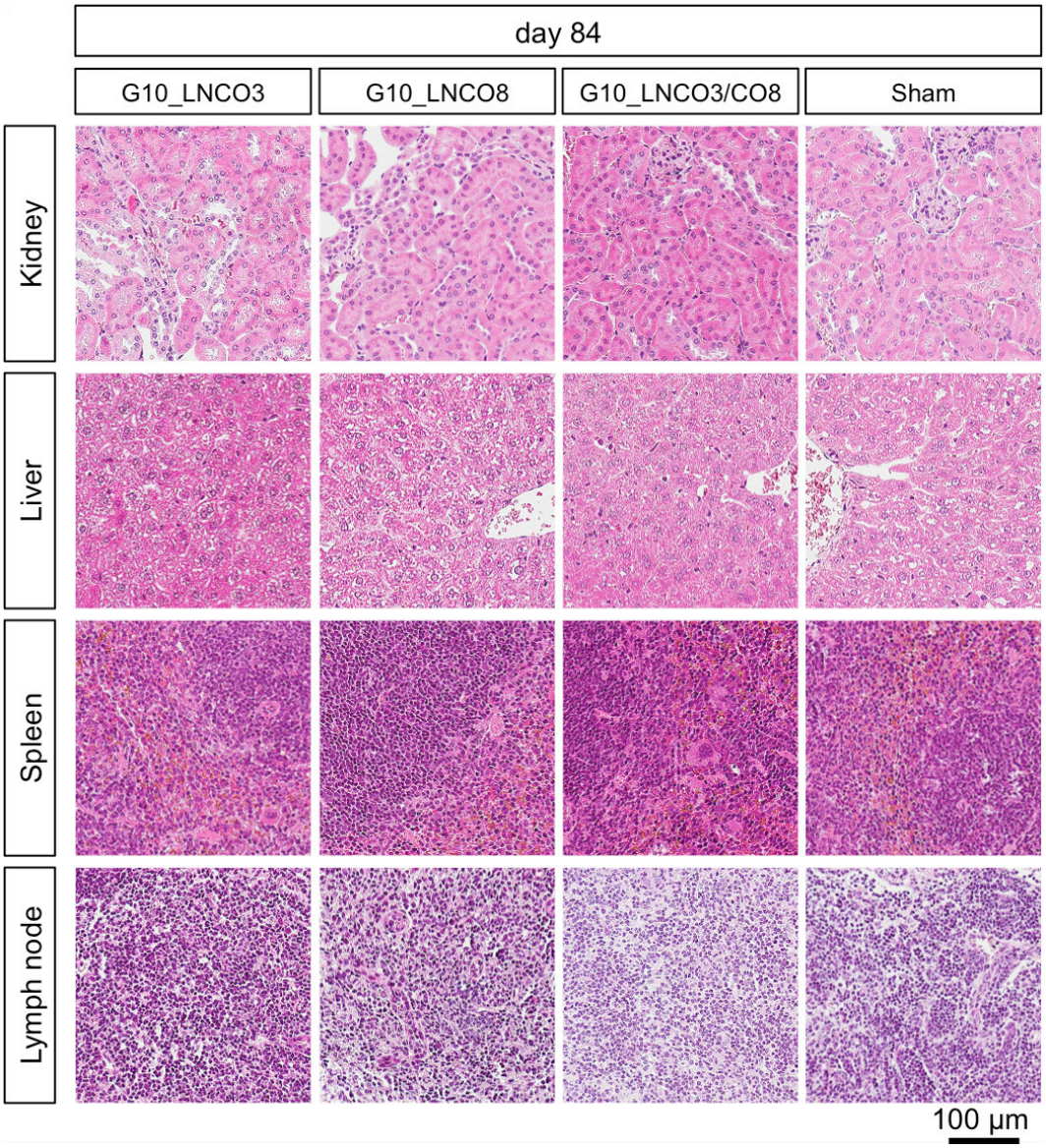

Fig. S7 Representative histological images of pathological examination. Pathological examination of kidney, liver, spleen and inguinal lymph nodes 84 days after single implantation with G10_LNCO3 or G10_LNCO8 or double implantation. Exemplary images of Hematoxylin & Eosin (H&E) stained tissue are shown.